J|A|C|S
ARTICLES
Published on Web 03/23/2006

A New Photostable Terrylene Diimide Dye for Applications in Single Molecule Studies and Membrane Labeling

Christophe Jung,[†] Barbara K. Müller,[†] Don C. Lamb,[†,‡] Fabian Nolde,[§] Klaus Müllen,[§] and Christoph Bräuchle*,[†]

Contribution from the Department für Chemie und Biochemie and Center for Nanoscience (CeNS), Ludwig-Maximilians-Universität, Butenandtstrasse 11, D-81377, München, Germany, Department of Physics, 1110 West Green Street, University of Illinois at Urbana-Champaign, Urbana, Illinois 61801-3080, and Max Planck Institut für Polymerforschung, Mainz, Germany

Received January 17, 2006; E-mail: Christoph.Braeuchle@cup.uni-muenchen.de

Abstract: A new terrylene diimide-based dye (WS-TDI) that is soluble in water has been synthesized, and its photophysical properties are characterized. WS-TDI forms nonfluorescing H-aggregates in water that show absorption bands being blue-shifted with respect to those of the fluorescing monomeric form. The ratio of monomeric WS-TDI to aggregated WS-TDI was determined to be 1 in 14 400 from fluorescence correlation spectroscopy (FCS) measurements, suggesting the presence of a large amount of soluble, nonfluorescent aggregates in water. The presence of a surfactant such as Pluronic P123 or CTAB leads to the disruption of the aggregates due to the formation of monomers in micelles. This is accompanied by a strong increase in fluorescence. A single molecule study of WS-TDI in polymeric films of PVA and PMMA reveals excellent photostability with respect to photobleaching, far above the photostability of other common water-soluble dyes, such as oxazine-1, sulforhodamine-B, and a water-soluble perylenediimide derivative. Furthermore, labeling of a single protein such as avidin is demonstrated by FCS and single molecule photostability measurements. The high tendency of WS-TDI to form nonfluorescent aggregates in water in connection with its high affinity to lipophilic environments is used for the fluorescence labeling of lipid membranes and membrane containing compartments such as artificial liposomes or endosomes in living HeLa cells. The superior fluorescence imaging quality of WS-TDI in such applications is demonstrated in comparison to other well-known membrane staining dyes such as Alexa647 conjugated with dextran and FM 4-64 lipophilic styryl dye.

Introduction

During the last few years, the interest in new water-soluble fluorescent dyes as labels for biological systems has strongly increased.[1−5] Many commercially available fluorescent dyes, such as rhodamines, cyanines, oxazines, and so forth, are water-soluble and fulfill additional requirements of a good fluorophore, such as high extinction coefficient, high fluorescence quantum yield, and good chemical stability. However, their photostability is limited, photobleaching after 10^4 to 10^6 photocycles. This is of particular disadvantage for single molecule studies where photobleaching severely limits the observation time and, thus, the amount of collected information during the experiment. Single molecule methods play a growing role in biophysical studies because they can reveal dynamics and mechanistic behavior that would be otherwise obscured by ensemble averaging in conventional spectroscopic techniques.[6−12]

Furthermore, fluorescent dyes are often used in "live cell imaging" experiments where single proteins, virions, drugs, or other single bioparticles are labeled so that they can be followed along pathways and/or interactions inside the living cell.[13−16] For live-cell imaging experiments, dyes that absorb and fluoresce above 600 nm are highly desirable as the background coming from the autofluorescence of living cells is negligible in this region. Up to now, there were very few, if any, water-soluble fluorophores with high photostability available in this spectral region.

[†] Ludwig-Maximilians-Universität.
[‡] University of Illinois at Urbana-Champaign.
[§] Max Planck Institut für Polymerforschung.

(1) Haugland, R. P. *The Handbook: A Guide to Fluorescent Probes and Labeling Technologies*, 10th ed.; Invitrogen: Eugene, OR, 2005.
(2) Brismar, H.; Trepte, O.; Ulfhake, B. *J. Histochem. Cytochem.* **1995**, *43*, 699−707.
(3) Panchuk-Voloshina, N.; Haugland, R. P.; Bishop-Stewart, J.; Bhalgat, M. K.; Millard, P. J.; Mao, F.; Leung, W. Y. *J. Histochem. Cytochem.* **1999**, *47*, 1179−1188.
(4) Margineanu, A.; Hofkens, J.; Cotlet, M.; Habuchi, S.; Stefan, A.; Qu, J. Q.; Kohl, C.; Mullen, K.; Vercammen, J.; Engelborghs, Y.; Gensch, T.; De Schryver, F. C. *J. Phys. Chem. B* **2004**, *108*, 12242−12251.
(5) Kapanidis, A. N.; Weiss, S. *J. Chem. Phys.* **2002**, *117*, 10953−10964.
(6) Michalet, X.; Kapanidis, A. N.; Laurence, T.; Pinaud, F.; Doose, S.; Pflughoefft, M.; Weiss, S. *Annu. Rev. Biophys. Biomol. Struct.* **2003**, *32*, 161−182.
(7) Weiss, S. *Nat. Struct. Biol.* **2000**, *7*, 724−729.
(8) Ha, T. *Methods* **2001**, *25*, 78−86.
(9) Michalet, X.; Weiss, S. *C. R. Phys.* **2002**, *3*, 619−644.
(10) Haustein, E.; Schwille, P. *Curr. Opin. Struct. Biol.* **2004**, *14*, 531−540.
(11) Peterman, E. J. G.; Sosa, H.; Moerner, W. E. *Annu. Rev. Phys. Chem.* **2004**, *55*, 79−96.
(12) Yildiz, A.; Forkey, J. N.; McKinney, S. A.; Ha, T.; Goldman, Y. E.; Selvin, P. R. *Science* **2003**, *300*, 2061−2065.
(13) Lippincott-Schwartz, J.; Snapp, E.; Kenworthy, A. *Nat. Rev.* **2001**, *2*, 444−456.
(14) Seisenberger, G.; Ried, M. U.; Endress, T.; Büning, H.; Hallek, M.; Bräuchle, C. *Science* **2001**, *294*, 1929−1932.
(15) Bräuchle, C.; Seisenberger, G.; Endress, T.; Ried, M. U.; Büning, H.; Hallek, M. *ChemPhysChem* **2002**, *3*, 299−303.

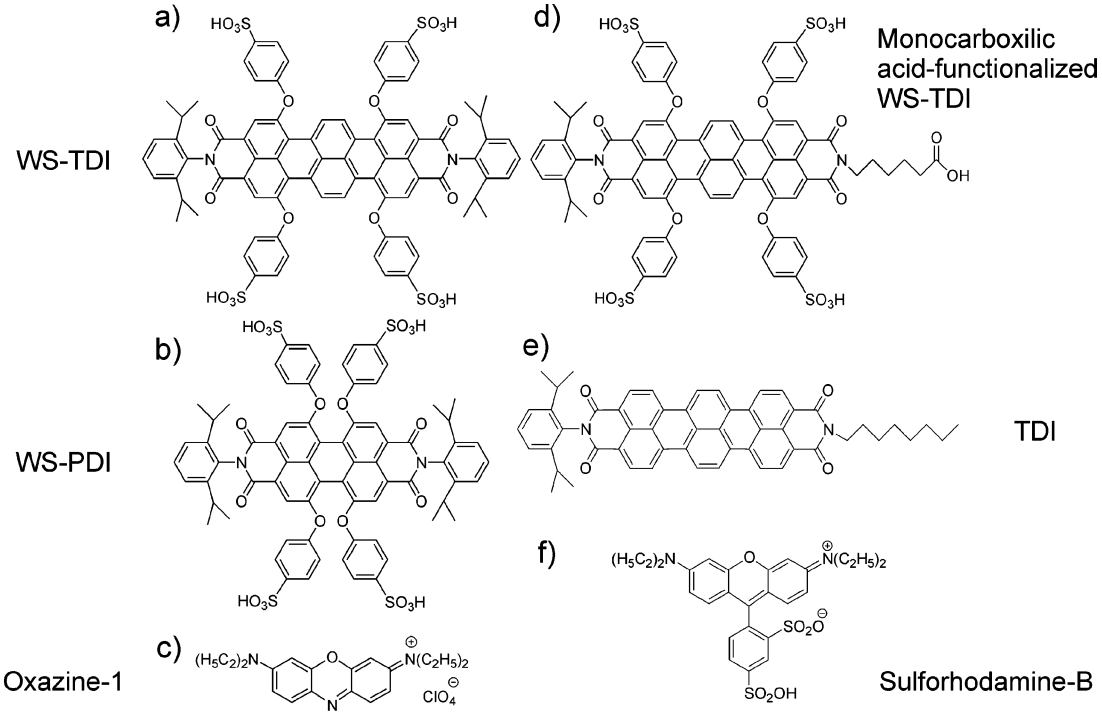

Figure 1. Structure of (a) 1,6,9,14-tetra(4-sulfonylphenoxy)-*N*,*N*′-(2,6-diisopropylphenyl)-terrylene-3,4:11,12-tetracarboxidiimide (WS-TDI), (b) 1,6,7,12-tetra(4-sulfonylphenoxy)-*N*,*N*′-(2,6-diisopropylphenyl)-perylene-3,4:9,10-tetracarboxidiimide (WS-PDI), a water-soluble terrylenediimide derivative, (c) oxazine-1, (d) 1,6,9,14-tetra(4-sulfonylphenoxy)-*N*-(2,6-diisopropylphenyl)-*N*′-(5-carboxpentyl)-terrylene-3,4:11,12-tetracarboxidiimide, a monocarboxylic acid-functionalized WS-TDI (e) *N*-(2,6-Diisopropylphenyl)-*N*′-(n-octyl)-terrylene-3,4:11,12-tetracarboxidiimide (TDI), and (f) sulforhodamine-B.

Rylene derivatives are known for their exceptional photophysical and photochemical stability as well as for their high fluorescence quantum yield, which is close to unity in organic solvents.[17,18] Unfortunately, they are not water-soluble. Water solubility can be obtained by introducing hydrophilic substituents onto the hydrophobic skeleton of these molecules. In many cases, fluorescence is strongly diminished because of the additional flexibility of the side groups which enhance the nonradiative decay channels. Furthermore, aggregation due to the hydrophobic core of such chromophores can lead to the quenching of the fluorescence. Sulfonation decreases the tendency to form aggregates, presumably due to increased polarity induced by the sulfonic acid group and due to steric effects. A perrylenediimide chromophore containing four charged sulfonyl groups (Figure 1b) has recently been synthesized,[19] and its photophysical properties have been characterized.[4] It is water-soluble, highly fluorescent, and very photostable. However, the absorption region of perylene dyes lies below 600 nm, whereas terrylene dyes absorb far above this wavelength. In addition, our experience shows that terrylene is even more photostable than perylene. Therefore, water-soluble terrylene derivatives should be an even more ideal fluorophore for single molecule and live-cell imaging experiments. The chemical structure of the water-soluble terrylene dye, 1,6,9,14-tetra(4-sulfonylphenoxy)-*N*,*N*′-(2,6-diisopropylphenyl)-terrylene-3,4:11,12-tetracarboxidiimide (WS-TDI), characterized in this study is shown in Figure 1a.

As will be demonstrated later in more detail, this molecule shows a nicely balanced effect of the hydrophilic sulfonic groups and the hydrophobic core. The sulfonic groups are responsible for the water solubility; however, due to the large π-electron system of the rigid hydrophobic core, many of the molecules are still stacked, forming water-soluble aggregates. The ambivalent nature of this molecule offers additional interesting properties since the terrylene core presents a strong affinity to, for example, lipid membranes. This property makes WS-TDI an exceptional label for artificial as well as biological membranes.

Here, we report on the photophysical properties and aggregation behavior of WS-TDI in purely aqueous media and in the presence of surfactants. The absorption and the fluorescence behavior strongly depends on the extent of aggregation and, thus, on the solvent used. A single molecule study of the photostability is also conducted to compare WS-TDI to other dyes and to establish its outstanding properties. In addition, the ability to label proteins with this dye is demonstrated using fluorescence correlation spectroscopy (FCS) measurements. Furthermore, the possibility of labeling artificial and natural membranes is investigated and shows, for example, the exceptional imaging properties of this dye for lipid membrane compartments in living cells.

Experimental Section

The WS-TDI was synthesized as described previously.[20]

UV−Visible Absorption and Fluorescence Spectroscopy. UV−visible measurements were performed with a Cary 50 Conc spectrophotometer (Varian), and fluorescence spectra measurements were performed with a F900 luminescence spectrometer (Edinburgh Analytical Instruments). Particle sizes were measured by laser-light scattering

(16) Schutz, G. J.; Sonnleitner, M.; Hinterdorfer, P.; Schindler, H. *Mol. Membr. Biol.* **2000**, *17*, 17−29.
(17) Dubois, A.; Canva, M.; Brun, A.; Chaput, F.; Boilot, J. P. *Appl. Opt.* **1996**, *35*, 3193−3199.
(18) Seybold, G.; Wagenblast, G. *Dyes Pigm.* **1989**, *11*, 303−317.
(19) Qu, J.; Kohl, C.; Pottek, M.; Müllen, K. *Angew. Chem.* **2004**, *116*, 1554−1557.
(20) Nolde, F.; Qu, J.; Kohl, C.; Pschirer, N. G.; Reuther, E.; Müllen, K. *Chem.−Eur. J.* **2005**, *11*, 3959−3967.

using a Malvern Zetasizer 3000HS (Malvern Instruments, Worcestershire, UK). Quantum yields of fluorescence were measured by comparing the fluorescence intensity of the sample to that of optically dilute solutions of Cy5 in Millipore water ($\varphi_f = 0.27$).[21] In the quantum yield experiments, changes in the absorption coefficient upon addition of Pluronic P123 or CTAB were compensated for by shifting the excitation wavelength to keep the same total absorption of the sample. Excitation wavelengths varied between 640 and 655 nm.

Confocal Microscopy. To investigate the photostability on a single molecule level, the dyes were embedded in polymer matrixes. Two different polymers were used: poly(vinyl alcohol) (PVA) and poly(methyl methacrylate) (PMMA). Thin polymer films (100−200 nm) were prepared by spin-coating fluorophores in polymer solutions at a concentration of 10^{-9} mol/L (1 min at 1000 rpm, 2 wt %/wt PVA in water; 1 min at 3000 rpm, 2 wt %/wt PMMA in chloroform). In addition to the photostability of WS-TDI, the photostability of four other dyes was investigated: 1,6,7,12-tetra(4-sulfonylphenoxy)*N*,*N*′-(2,6-diisopropylphenyl)-perylene-3.4:9,10-tetracarboxidiimide (WS-PDI) (Figure 1b), oxazine-1 (Figure 1c), *N*-(2,6-Diisopropylphenyl)-*N*′-(n-octyl)-terrylene-3,4:11,12-tetracarboxidiimide (TDI) (Figure 1e), and sulforhodamine-B (Figure 1f). Sulforhodaine-B and oxazine-1 were purchased commercially (Lambdachrome). WS-PDI and sulforhodamine-B have similar absorption spectra (data not shown) and were excited with a continuous wave (cw) krypton-ion laser (568 nm). The maximum of fluorescence emission was observed at around 610 nm. WS-TDI, TDI, and oxazine-1 were excited with a cw He−Ne laser (633 nm) and had the maximum of fluorescence emissions at approximately 700 nm. A modified scanning confocal microscope (ZEISS LSM 410) was used to visualize fluorescence of the individual dye molecules. High spatial resolution and detection efficiency were achieved with a high-numerical aperture oil-immersion objective (ZEISS 40 × 1.3 NA oil). Using circular polarized excitation light, all in-plane molecular absorption dipoles are excited with the same probability. The fluorescence emission of WS-PDI and suforhodamine-B were separated from the excitation laser beam using a 575LP dichroic filter (AHF Analysentechnik) and an emission filter (HQ655/150, AHF Analysentechnik). Red-shifted fluorescence was separated from backscattered laser light by a combination of a dichroic mirror (Q640LP AHF Analysentechnik), a notch filter (633 nm Notch Kaiser), and an emission filter (HQ720/150 AHF Analysentechnik). The fluorescence signal was detected by an avalanche photodiode (APD, EG&G SPCM-AQ 141). The excitation power at the entrance of the objective was set to 18 μW.

With the confocal setup, the laser beam could be positioned over individual molecules, and their fluorescence intensities were recorded with time. Two photostability parameters could be automatically extracted from the fluorescence time trajectories of individual molecules by a custom-written LabView program: the number of detected photons before photobleaching as the integral over a time trace and the survival time, which is the total duration of the time trace until photobleaching. The total detection efficiency of our experimental setup is estimated to be 2.5% and was used to calculate the total number of emitted photons.

Data Analysis. The analysis of the photostability parameters was based on calculating the probability distributions of the number of total emitted photons (TEP) before photobleaching and of the survival times (ST).[22] Analyzing probability distributions instead of histograms allows for a more precise analysis, avoiding loss of information due to binning of the histogram, and mono- and biexponential decays can be better distinguished. The distributions in TEP and ST are well approximated by a multiexponential function, $S(t)$, which is defined by characteristic decay parameters

$$S(t) = \sum_{i=0}^{n} A_i \exp\left(-\frac{t}{\tau_i}\right) \tag{1}$$

where τ_i is the decay time and A_i is the amplitude of the individual components.

The number of exponential components was determined by the decrease in the reduced χ^2 of the fit function. A minimum 2-fold decrease in the reduced χ^2 of the fit was required to justify an additional exponential decay in the model function.[23] For all results presented in this article, a biexponential function was found to give the best fit with the exception of TDI, where a monoexponential was sufficient to fit both the TEP and the ST. For comparison of the photobleaching behavior between the different dyes, an average TEP or ST, represented by $\langle\tau\rangle$, was defined as:

$$\langle\tau\rangle = \sum_{i=0}^{n} A_i \cdot \tau_i \tag{2}$$

Synthesis of Monocarboxylic Acid-Functionalized WS-TDI. The monocarboxylic acid-functionalized terrylenediimide was synthesized by using *N*-(5-carboxypentyl)-naphthalenedicarboximide and a perylenedicarboximide in the one-pot synthesis (*t*-BuONa/DBN, diglyme) of terrylenediimide.[20] Bromination of this terrylenediimide with elemental bromine in chloroform gives the corresponding tetrabrominated terrylenediimide. The substitution under basic conditions of the four bromine atoms with phenol and subsequent sulfonation with concentrated sulfuric acid at room temperature affords the monocarboxylic acid-functionalized WS-TDI (1,6,9,14-tetra(4-sulfonylphenoxy)-*N*-(2,6-diisopropylphenyl)-*N*′-(5-carboxpentyl)-terrylene-3,4:11,12-tetracarboxidiimide). The structure is shown in Figure 1d.

Protein Labeling. Terrylenediimide monocarboxylic acid was used to label the amine group of exposed lysine residues of avidin. The avidin protein was dissolved at a concentration of 10 mg/mL in phosphate-buffered saline (PBS) buffer. The monocarboxylic acid-functionalized terrylenediimide to be coupled was dissolved in the same buffer. The dye solution was added to the protein solution in a 10 M excess. A 1-ethyl-3-[3-dimethylaminopropyl] carbodiimide hydrochloride (EDC) solution was added to obtain a 20-fold molar excess of EDC to the protein. The cross-linking reaction was performed in an Eppendorf tube. The tube was shaken on a test tube shaker for 4 h at 30 °C.

Microbiospin chromatography was used to purify the labeled avidin form unbound WS-TDI. A volume of 50 μL of the reaction mixture was applied to a microspin column (Microspin G-50 column, Amersham) and centrifuged for 2 min at 3000 rpm. The procedure was repeated a second time to increase the purity of the labeled protein sample.

Fluorescence Correlation Spectroscopy and Fluorescence Lifetime Measurements. FCS and fluorescence lifetime measurements were performed using a home-built confocal setup. Details of the setup can be found in Müller et al.[24] Briefly, the system is built around an inverted microscope (Axiovert200, Zeiss, Göttingen, Germany). The laser (LDH-P-C-635 and Sepia PDL808, PicoQuant, Berlin, Germany) was guided through a single-mode polarization-maintaining fiber (PMJ-3AF3AF-633-4/125-3-5-1, OZ Optics, Carp, Ontario, Canada) before entering the microscope and focusing on the sample by a water immersion objective (C-Apochromat, 63 × 1.2, Zeiss, Göttingen, Germany). The fluorescence was collected by the same objective and separated from the excitation beam by a dichroic mirror (DC532/633xr, AHF Analysentechnik, Tübingen, Germany). After passing an emission filter (HQ700/75, AHF Analysentechnik), the fluorescence was focused on a pinhole (50 μm, Owis, Staufen, Deutschland) and finally on an avalanche photodiode (SPCM-AQR-14, EG&G Optoelectronics, Vaudreuil, Quebec, Canada). The data were recorded by a digital real-time correlator (ALV GmbH, Langen, Germany) or time-correlated single-photon counting card (TimeHarp 200, PicoQuant, Berlin, Germany).

(21) Mujumdar, R. B.; Ernst, L. A.; Mujumdar, S. R.; Lewis, C. J.; Waggoner, A. S. *Bioconjugate Chem.* **1993**, *4*, 105−111.
(22) Molski, A. *J. Chem. Phys.* **2001**, *114*, 1142−1147.
(23) Lakowicz, J. R. *Principles of Fluorescence Spectroscopy*, 2nd ed.; Plenum Press: New York, 1999; pp 129−130.
(24) Müller, B. K.; Zaychikov, E.; Bräuchle, C.; Lamb, D. C. *Biophys. J.* **2005**, *89*, 3508−3522.

The autocorrelation function, G_D, was calculated from the FCS measurements and fit with the three-dimensional Gaussian model for freely diffusing particles in solution:[25,26]

$$G_D(\tau) = \frac{\gamma}{\langle N \rangle}\left(\frac{1}{1+\tau/\tau_D}\right)\left(\frac{1}{1+(\omega_r/\omega_z)^2\tau/\tau_D}\right)^{1/2} \quad (3)$$

where γ is the geometrical correction factor (equal to $2^{-1.5}$), N is the average number of molecules in the detection volume, τ is the correlation time, ω_i is the radius of the laser focus in lateral (r) and axial (z) directions, respectively, to the distance where the intensity has decayed by a factor of $1/e^2$, and τ_D is the average diffusion time of a particle through the detection volume. $\tau_D = \omega_r^2/(4D)$, where D is the diffusion coefficient of the fluorescence particle. The volume of the setup was calibrated using freely diffusing Cy5 as a reference sample and assuming a diffusion coefficient of 250 $\mu m^2/s$.[27] The correlation functions where fit using Origin6.0 (OriginLab Corporation, Northampton, MA).

The lifetime measurements were performed on the same setup. Data were recorded with the time-correlated single-photon counting card and analyzed with PicoQuant FluoFit version3.0.

Liposome Labeling. Liposomes composed of 1,2-dipalmitoyl-*sn*-glycero-3-phosphocholine (DPPC), 1,2-distearoyl-*sn*-glycero-3-phosphocholine (DSPC), and 1,2-dipalmitoyl-*sn*-glycero-3-phosphoglycerol (DPPGOG) in a 5:2:3 molar ratio in*N*-[2-hydroxyethyl]piperazine-*N*′-[2-ethanesulfonic acid] (Hepes) buffered glucose were prepared as described in the literature.[28]

WS-TDI was incorporated into the membrane of the liposomes by incubation at room temperature for 1 h. The concentrations of WS-TDI and lipid in the liposome probe were, respectively, 0.1 and 32 mmol/L. WS-TDI-labeled vesicles were separated from noninserted fluorophores by spin chromatography on saccharose solution (20 wt %/wt) in Hepes buffer (14 000 rpm for 90 min at 4 °C). Before performing single molecule wide-field microscopy measurements with the labeled liposomes, the purified sample was diluted 500 times in Hepes buffer.

Live-Cell Measurements. HeLa cells (HeLa ACC57, DSMZ, Braunschweig, Germany) were grown in Dulbecco's modified Eagle's medium (DMEM) supplemented with 10% fetal calf serum at 37 °C in 5% CO_2 humidified atmosphere. Cell culture, fetal calf serum, and PBS buffer were purchased from Invitrogen GmbH (Karlsruhe, Germany). Dye-uptake experiments were conducted in HeLa cells at 37 °C. Solutions ($C \approx 4 \times 10^{-6}$ mol/L) of WS-TDI, Alexa 647/dextran, and *N*-(3-triethylammoniumpropyl)-4-(6-(4-(diethylamino)phenyl)-hexatrienyl)pyridinium dibromide (FM 4-64 styryl dye, Molecular Probes) were added to the cells adherent on the surface of a cover glass. After an incubation time of about 40 min, the solutions were washed out 4 times with PBS buffer to remove the excess dye.

The fluorescence signal from labeled liposomes and HeLa cells was monitored by epifluorescence microscopy with a wide-field imaging setup. The dye was excited with a He−Ne laser (NEC) at 633 nm, or a Nd:YAG laser (Soliton) at 532 nm. The excitation powers were set to 1.7 mW at the entrance of the microscope. The laser beams were expanded and focused onto the back-focal plane of a microscope objective (Nikon Plan Apo 100×/1.4 oil; the microscope stand was a Nikon eclipse TE200). Fluorescence was collected by the same objective, separated from backscattered laser light with a combination of filters (dicroic mirror 640 nm cutoff and band-pass BP730/140 AHF), and imaged onto a back-illuminated CCD detector (Andor, iXon DV897). Movies were recorded with a resolution of 122 nm per pixel and an integration time of 100 ms per frame for the diffusion measurements of liposomes in Hepes buffer, and 500 ms per frame for the measurements with HeLa cells.

Results and Discussion

Absorption and Emission Spectra. The spectral and luminescence properties of WS-TDI depend substantially on the environment. This is due to the favorability of forming aggregates in polar media, such as water, while WS-TDI remains monomeric in other solvents such as dimethyl sulfoxide (DMSO).

The absorption and emission spectra of WS-TDI dissolved in DMSO with a concentration of $C = 10^{-5}$ mol/L are shown in Figure 2a (solid lines). Two distinct absorption bands can be assigned to two different electronic transitions in the monomeric molecule, the S_0-S_1 from 550 to 720 nm and the S_0-S_2 from 390 to 460 nm.[29]

The S_0-S_1 presents a maximum at 677 nm with a molar extinction coefficient of 36 800 M^{-1} cm^{-1}. The Stokes shift of fluorescence emission is 43 nm, while the quantum yield of fluorescence is $\varphi_f = 0.08$ in DMSO. In addition, time-resolved measurements have been performed to investigate the photophysical parameters of this dye. The fluorescence decay of a 10^{-5} mol/L WS-TDI solution in DMSO was monoexponential with a lifetime of $\tau = 0.88 \pm 0.01$ ns. From the quantum yield $\varphi_f = k_f/(k_f + k_{nr})$, where k_f is the fluorescence rate constant and k_{nr} is the nonradiative rate constant, and the lifetime $\tau = 1/(k_f + k_{nr})$, we obtain $k_f = 8.9 \times 10^7$ s^{-1} and $k_{nr} = 1.0 \times 10^9$ s^{-1}. Hence, $k_{nr} \gg k_f$.

In contrast to the data in DMSO, the absorption spectrum of WS-TDI in water (dotted line, Figure 2b) consists of a main band at a shorter wavelength of 637 nm and a weak band at 690 nm. Nearly no fluorescence emission signal is observed in the region of the fluorescence spectrum (dotted line, Figure 2d, excitation 645 nm).

Self-association of dyes in solution is a frequently encountered phenomenon in dye chemistry owing to strong intermolecular forces.[30,31] WS-TDI is a relatively rigid molecule with a large planar π-electron system with hydrophobic nature and has a strong tendency to aggregate in polar solvents such as water. Previous studies have already characterized aggregates of $\pi-\pi$ stacked perylene diimide dyes in solution,[32] which have a slightly smaller π-electron system than WS-TDI.

In general, aggregates in solution exhibit distinct changes in absorption and fluorescence properties compared to that in monomeric species. Molecular excitonic theory describes two main species of dye aggregates distinguished as H- and J-aggregates (Figure 2c). H-Aggregates are formed by parallel stacking, whereas J-aggregates occur in a head-to-tail arrangement.[33,34] In H-aggregates, the absorption maximum is blue-shifted with respect to the isolated chromophore and the fluorescence is normally quenched. However, J-aggregates usually show fluorescence, and both the absorption and emission maxima are red-shifted.[35] Comparing these statements with our observations, we conclude that WS-TDI forms H-aggregates in water.

(25) Elson, E. L.; Magde, D. *Biopolymers* **1974**, *13*, 1−27.
(26) Thompson, N. L. Fluorescence Correlation Spectroscopy. In *Topics in Fluorescence Spectroscopy*; Lakowicz, J. R., Ed.; Plenum Press: New York, 1991; Vol. 1, pp 337−378.
(27) Widengren, J.; Schwille, P. *J. Phys. Chem. A* **2000**, *104*, 6416−6428.
(28) Lindner, L. H.; Eichhorn, M. E.; Eibl, H.; Teichert, N.; Schmitt-Sody, M.; Issels, R. D.; Dellian, M. *Clin. Cancer Res.* **2004**, *10*, 2168−2178.
(29) Gvishi, R.; Reisfeld, R.; Burshtein, Z. *Chem. Phys. Lett.* **1993**, *213*, 338−344.
(30) Brichkin, S. B.; Kurandina, M. A.; Nikolaeva, T. M.; Razumov, V. F. *High Energy Chem.* **2004**, *38*, 373−380.
(31) Das, S.; Thomas, K. G.; Thomas, K. J.; Madhavan, V.; Liu, D.; Kamat, P. V.; George, M. V. *J. Phys. Chem.* **1996**, *100*, 17310−17315.
(32) Würthner, F.; Thalacker, C.; Diele, S.; Tschierske, C. *Chem.−Eur. J.* **2001**, *7*, 2245−2253.
(33) Kasha, M.; Rawls, H. R.; El-Bayoumi, M. A. *Pure Appl. Chem.* **1965**, *11*, 371−392.
(34) McRae, E. G.; Kasha, M. *J. Chem. Phys.* **1958**, *28*, 721−722.

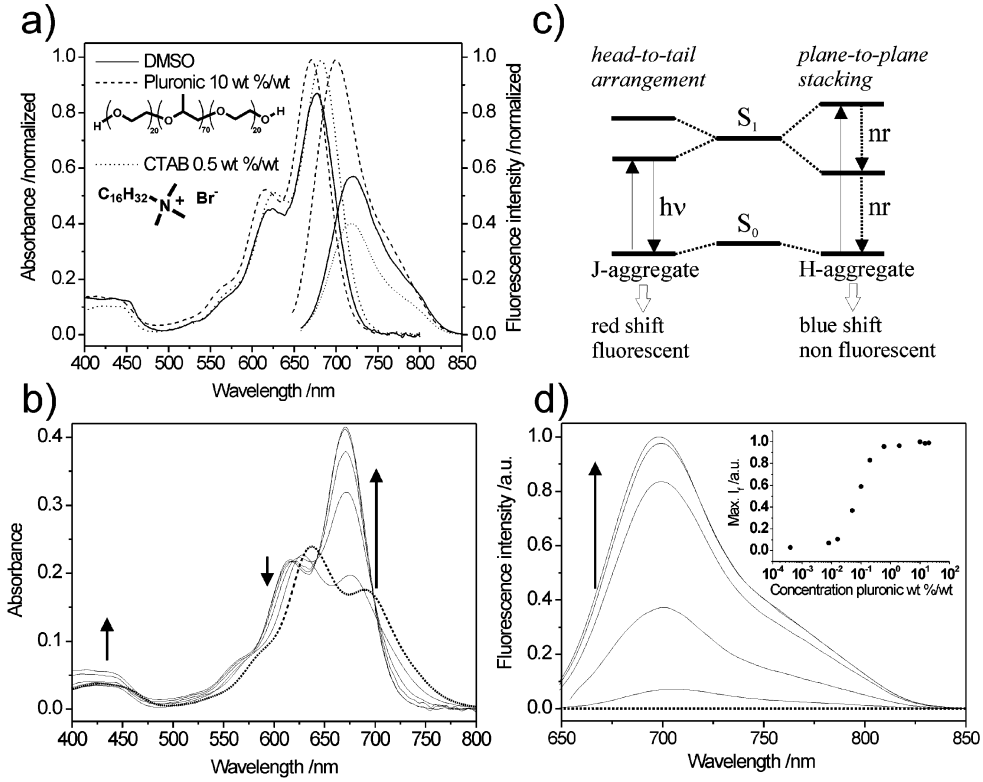

Figure 2. (a) Absorption spectra of 10^{-5} mol/L WS-TDI solutions in DMSO (continuous line), in water in the presence of 10 wt %/wt Pluronic P123 (dashed line), in water in the presence of 0.5 wt %/wt CTAB (dotted line), and their corresponding fluorescence spectra (λ_{ex} = 655, 643, and 653 nm, respectively). The spectra are normalized to the absorption and fluorescence maxima of WS-TDI in water taken in the presence of 10 wt %/wt Pluronic P123. Schematic structures of Pluronic P123 and CTAB are shown in the inset. (b) Effect of Pluronic concentration on the absorption spectrum of WS-TDI in water ($C = 10^{-5}$ mol/L). The broken line represents the absorption spectrum of WS-TDI in water without addition of surfactant. The solid lines represent a titration with Pluronic P123. Arrows indicate the direction of change with increasing Pluronic concentration (0.008, 0.05, 0.2, 2, and 20 wt %/wt, respectively). (c) Schematic diagram of H- and J-aggregates and their influence on the energy levels and fluorescence behavior of WS-TDI. (d) Normalized fluorescence emission spectra (λ_{ex} = 640−650 nm) corresponding to the absorption spectra in panel b. Inset shows the plot of the maximum of fluorescence intensity versus Pluronic 123 concentration.

Light scattering measurements show the presence of particles of a size of 449 ± 53 nm at a WS-TDI concentration of 10^{-5} mol/L in water, whereas no signal from light scattering is detected in DMSO at the same WS-TDI concentration. Moreover, the size of the aggregates in water decreases with diminishing dye concentration (472 ± 117 nm at 10^{-4} mol/L and 114 ± 24 nm at 10^{-6} mol/L). This is a typical observation of dye aggregation in water solution, whereas in DMSO, no light scattering signal was detected, suggesting that no aggregation takes place.

Further measurements were conducted in the presence of the nonionic block copolymer surfactant poly(ethylene oxide)−poly(propylene oxide)−poly(ethylene oxide) (Pluronic P123, BASF), at different surfactant concentrations for a 10^{-5} mol/L WS-TDI concentration in water. The absorption and fluorescence spectra are shown in Figure 2b,d. The concentration of Pluronic P123 was increased from 0.0004 to 20 wt %/wt. A pronounced reduction in the intensity of the band absorbing near 630 nm in favor of the band at longer wavelength (670 nm) is observed with increasing concentration of Pluronic P123. Moreover, a small fluorescence signal already appears with the lowest concentration of Pluronic P123. The fluorescence intensity increases dramatically with higher surfactant concentrations. The inset in Figure 2d shows the fluorescence intensity as a function of Pluronic P123 concentration. The fluorescence intensity is near zero with the WS-TDI in water and increases drastically for surfactant concentrations above 0.04 wt %/wt. This concentration corresponds to the critical micelle concentration (CMC) of Pluronic P123[36] (i.e., the starting point of the formation of micelles). The fluorescence intensity saturates for surfactant concentration above about 2%.

Furthermore, the measurements of the size of the particles by light scattering in a solution of WS-TDI in the presence of 2 and 10% Pluronic show the presence of particles with a diameter of 9 ± 3 and 18 ± 3 nm, respectively, which is the diameter of the hydrophobic micelles themselves formed by Pluronic at these concentrations.[37] No light scattering signal is detectable anymore at a particle diameter around 449 nm, which was observed for pure water solutions of WS-TDI at the same concentration. In addition, a similar shape of the absorption spectra of WS-TDI in DMSO and in water in the presence of Pluronic above CMC is observed, as illustrated in Figure 2a. These results suggest that WS-TDI molecules are incorporated into micelles and that most of the molecules are present in a monomeric form associated with the hydrophobic micelles. The extinction coefficient of this monomeric absorption band (670 nm) in the presence of 10 wt %/wt of Pluronic is estimated to be 42 000 M^{-1} cm^{-1}. The corresponding quantum yield of fluorescence (φ_f) is equal to 0.17.

(35) Franck, J.; Teller, E. *J. Chem. Phys.* **1938**, *6*, 861−872.
(36) Alexandridis, P.; Holzwarth, J. F.; Hatton, T. A. *Macromolecules* **1994**, *27*, 2414−2425.
(37) Hioka, N.; Chowdhary, R. K.; Chansarkar, N.; Delmarre, D.; Sternberg, E.; Dolphin, D. *Can. J. Chem.* **2002**, *80*, 1321−1326.

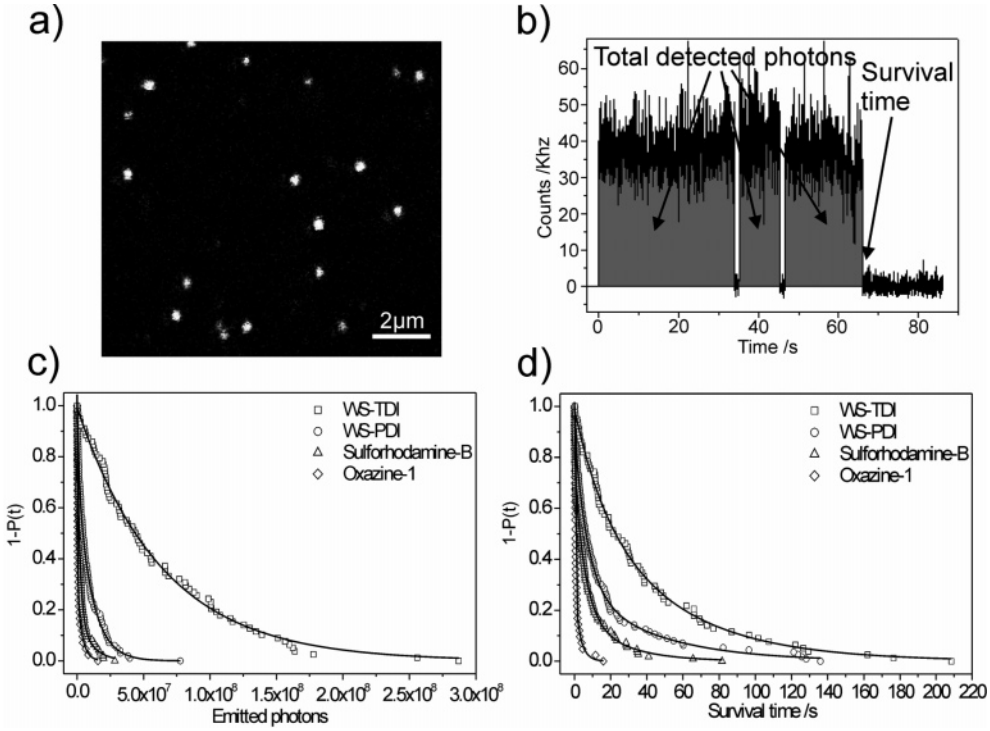

Figure 3. (a) Fluorescence image of single WS-TDI molecules embedded in PVA. (b) A typical fluorescence intensity trajectory. The molecule shows blinking behavior and undergoes irreversible photobleaching. (c) Accumulated probability distributions of the TEP for WS-TDI (□), WS-PDI (○), sulforhodamine-B (△), and oxazine-1 (◇). The curves cannot be fitted with a single component exponential decay. Instead, two-component decays were used and are shown as solid lines. (d) The same evaluation for the ST with biexponential fits shown as solid lines.

The absorption and emission spectra of a WS-TDI solution ($C = 10^{-5}$ M) in the presence of the cationic surfactant cetyltrimethylammonium bromide (CTAB) at a concentration 0.5 wt %/wt, much higher than the CMC of ~0.03 wt %/wt, are compared to the spectra of the dye in DMSO and in water in the presence of 10% of Pluronic (Figure 2). Addition of CTAB leads to shifts in the absorption and emission maxima to 682 and 718 nm, respectively. This is accompanied by a decrease in the fluorescence quantum yield of WS-TDI ($\varphi_f = 0.05$) compared to the hydrophobic Pluronic environment. However, the absorption spectrum is very similar to those in DMSO and in water in the presence of 10 wt %/wt Pluronic. In particular, the ratios of the intensities of the two adsorption bands around 675 and 630 nm are the same in all three cases. No signal was obtained by light scattering measurements. It is expected that micelles of CTAB are smaller than those formed by Pluronic due to the shorter hypdophobic chains of CTAB[38] and may be below the detection limit of our setup. More important, the peak of particle sizes around 449 nm found in pure water vanishes, indicating that WS-TDI is present only in the monomeric form, solubilized in micelles of CTAB. All spectral and photophysical data of this section are summarized in Table 1.

Table 1. Photophysical Parameters for WS-TDI in Different Solvents

solvent	λ_{abs}^{max} (nm)	λ_{em}^{max} (nm)	ϵ_{max} (M^{-1} cm^{-1})	Φ_f	particle size (nm)
DMSO	677	720	36800	0.08	–
water	637	–	23900	–	449
water, 10 wt %/wt Pluronic	670	700	42000	0.17	18
water, 0.5 wt %/wt CTAB	682	718	41700	0.05	–

Single Molecule Studies. A common experimental approach in single molecule spectroscopy is to spatially resolve the fluorescence signals of immobilized single molecules. One way to immobilize and investigate single molecules is to dissolve highly diluted solutions in a polymer and spin coat a thin film of the polymer on a substrate. Under these conditions, the molecules are so widely separated that on average less than one molecule is in the confocal spot of the laser beam. Scanning the laser beam across the sample allows single molecules to be detected by their fluorescence (for details, see the Experimental Section). Figure 3a shows a typical example of a 11 × 12 μm^2 confocal fluorescence image of individual WS-TDI molecules embedded in a PVA film. Each bright spot represents a single fluorescent molecule. The fluorescent intensities of individual molecules are observed by positioning the laser beam on such a spot and collecting the emitted fluorescence as a function of time. A typical fluorescence intensity trajectory is shown in Figure 3b. This trajectory shows blinking events at 33 and 46 s and one-step photobleaching at 65 s. The digital on−off switching of the fluorescence intensity in the blinking and photobleaching behavior is a typical signature for a single molecule. From such a fluorescence intensity trajectory, the number of total emitted photons (TEP, gray area as integral over time in Figure 3b corrected by detection efficiency of the setup; see Experimental Section) and the survival time (ST, time to the irreversible photobleaching) can be extracted. The distributions of these two parameters characterize the fluorescence capability and the photostability of a fluorescent dye.

We have measured the fluorescence intensity trajectories of 79 single WS-TDI molecules. The resulting probability distribu-

(38) Rosen, M. J. *Surfactants and interfacial phenomena*, 2nd ed.; Wiley & Sons: New York, 1989.

Table 2. Average TEP and ST Parameters of Different Dyes in Spin-Coated PVA and PMMA

fluorophore	matrix	λ_{ex} (nm)	total emitted photons ($\times 10^6$)	survival time (s)
WS-TDI	PVA	633	63.7 ± 0.7	40.3 ± 1.2
WS-PDI	PVA	568	7.8 ± 0.4	14.7 ± 0.3
sulforhodamine-B	PVA	568	3.6 ± 0.1	7.7 ± 2.1
oxazine-1	PVA	633	1.2 ± 0.4	1.1 ± 0.3
WS-TDI	PMMA	633	109.9 ± 14.1	60.6 ± 3.7
WS-PDI	PMMA	568	11.1 ± 2.3	34.5 ± 2.1
TDI	PMMA	633	301.2 ± 18.5	98.0 ± 3.8

tions of TEP and ST for WS-TDI in PVA are plotted in Figure 3c,d (□). Molski[22] developed a formalism to calculate the TEP and ST and showed that those distributions are well approximated by either mono- or multiexponential distributions. Multiexponential distributions can be characterized by an average TEP and ST, as described in the Experimental Section.

Our experimental data were best fit with biexponential decays. Similar biexponential photobleaching kinetics have been reported for fluorescein in PVA and were tentatively attributed to the influence of dye−polymer interactions.[39] It should be noted that the photobleaching mechanisms and such multiexponential decays are presently not fully understood on a molecular level.[40]

The average TEP for WS-TDI in PVA is calculated to be $63.7 \pm 0.7 \times 10^6$, and the average ST gives 40.3 ± 1.2 s. The fluorescence capability and photostability of WS-TDI were compared with three other dyes studied under the same experimental conditions. The probability distributions for 99 molecules of WS-PDI, 96 molecules of sulforhodamine-B, and 43 molecules of oxazine-1, all dissolved in PVA, are shown in Figure 3c,d. The corresponding average TEP and ST are summarized in Table 2. WS-TDI emits about 8, 18, and 53 times more photons before photobleaching and lives 3, 5, and 37 times longer than WS-PDI, sulforhodamine-B, and oxazine-1, respectively. Our results for WS-PDI are in good agreement with the data reported by Margineanu et al.,[4] provided their detection efficiency is below 10% (the number, though reasonable, was unfortunately not given in their report).

Rhodamine and oxazine molecules are currently among the best performing water-soluble dyes to our knowledge. Our results clearly show that WS-TDI emits many more photons over a longer period of time than the other dyes we have measured. The high number of emitted photons and the superior photostability combined with the absorption in the red spectral region (650 nm, avoiding, for example, autofluorescence in live-cell imaging experiments) make this dye very promising for single molecule experiments.

To make a direct comparison between WS-TDI and TDI (which cannot be dissolved in water or PVA), we investigated the photostability of both dyes in PMMA. TDI has the same terrylene chromophore as WS-TDI and is currently the most photostable and best performing dye to our knowledge. Measurements on 71 WS-TDI molecules and 60 TDI molecules in PMMA yielded an average TEP of $110 \pm 14 \times 10^6$ and $301 \pm 19 \times 10^6$ and an average ST of 61 ± 4 and 98 ± 4 s for WS-TDI and TDI, respectively. The average TEP of WS-TDI is approximately one-third that of TDI, and the decrease is attributed to the lower fluorescence quantum yield of the dye due to the influence of the flexible and charged sulfonyl groups attached to the chromophore. The difference in ST is decreased by 40%. In a sense, the lower TEP and ST is the price one has to pay to make TDI water-soluble.

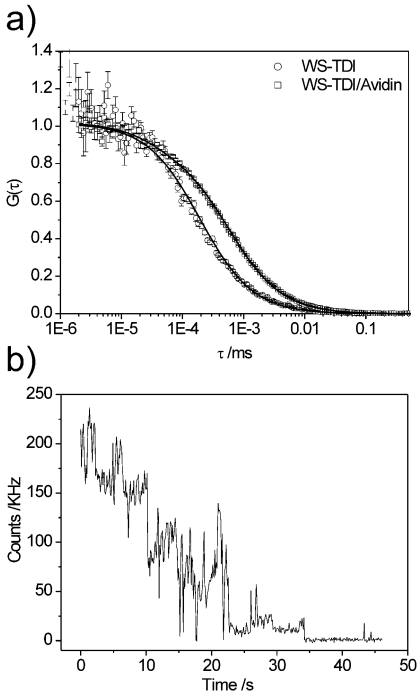

Figure 4. (a) Normalized autocorrelation curves of WS-TDI (○) and of WS-TDI-labeled avidin (□) in PBS. The shift of the curve of WS-TDI-labeled avidin to the right compared to the free dye indicates a lower diffusion coefficient in PBS. (b) Example of a fluorescence intensity trajectory of a WS-TDI-labeled avidin molecule. The stepwise decay reveals that several single WS-TDI molecules are bound to this protein.

PMMA has a stabilizing effect on WS-TDI, increasing the TEP by approximately 70% and the ST by 50%. The reason for the improvement in these parameters may be related to the lower polarity of PMMA. PVA matrix has a dielectric constant $\epsilon = 5.0$ in comparison to a value $\epsilon = 3.2$ for PMMA. The results of these measurements are summarized in Table 2.

Protein Labeling. The experiments described above show that WS-TDI is a promising dye for single molecule experiments due to its high photostability, red excitation spectrum, relatively high fluorescence quantum yield, and solubility in water. To be an effective fluorophore for biological applications, it is essential that the fluorophore can be used for labeling proteins. Thus, we modified the WS-TDI and used the new dye to stochastically label lysine residues on the surface of avidin. TDI monocarboxylic acid was mixed with avidin at a ratio of 10:1. The free dye was separated from labeled protein as discussed in the Experimental Section, and the labeled protein was investigated using FCS and single molecule fluorescence intensity measurements.

The normalized autocorrelation curves for WS-TDI (○) and WS-TDI/avidin (□) determined from FCS measurements in PBS are plotted in Figure 4a. The diffusion time is the average time a particle needs to diffuse across the confocal FCS volume. It is roughly the time at which the autocorrelation function has decayed to half of its initial amplitude. In Figure 4a, there is a clear shift to longer diffusion times for the WS-TDI−avidin

(39) Talhavini, M.; Atvars, T. D. Z. *J. Photochem. Photobiol., A* **1998**, *114*, 65−73.
(40) Zondervan, R.; Kulzer, F.; Kol'chenko, M. A.; Orrit, M. *J. Phys. Chem. A* **2004**, *108*, 1657−1665.

complexes, indicating that the mobility of WS-TDI is decreased by attachment to avidin and confirming that the protein has been successfully labeled. The exact values obtained from the fit of the curves with eq 2 are $\tau_D = 0.56$ μs for WS-TDI/avidin and $\tau_D = 0.19$ μs for WS-TDI, corresponding to diffusion coefficients of $D = 48$ $\mu m^2/s$ and $D = 140$ $\mu m^2/s$ for WS-TDI/avidin and WS-TDI, respectively. The three times lower diffusion coefficient of WS-TDI/avidin is expected due to the much larger hydrodynamic radius of WS-TDI/avidin. Avidin has a molecular weight of 67 kDa compared to 1.524 kDa for WS-TDI.

Moreover, the amplitude of the autocorrelation curve is proportional to the inverse number of fluorescent molecules in the confocal volume and can thus yield the concentration of the fluorescent species. FCS measurements were performed on a 3.6×10^{-5} mol/L concentration of WS-TDI in PBS. The amplitude of the autocorrelation function shown normalized to 1 in Figure 4a is 0.18, corresponding to an average of two fluorescent molecules in the confocal volume. Thus, the concentration of fluorescent WS-TDI in the probe volume of approximately 1.3 fL is $C_m = 2.5 \pm 0.2 \times 10^{-9}$ mol/L. Therefore, we can conclude that only about one molecule out of 14 400 is in the monomeric fluorescent form in the solution. This confirms the qualitative result previously found that the vast majority of the molecules form nonfluorescing aggregates in water and only a small monomeric fraction shows fluorescence.

The fluorescence intensity trajectory of a WS-TDI−avidin complex dissolved in PVA is shown in Figure 4b. The shape of this trace is in sharp contrast to the single molecule trace shown in Figure 3b. A stepwise decay is observed rather than the digital on and off states we observed previously. The behavior results from the combination of photoblinking and photobleaching of at least five WS-TDI molecules. As the sample is highly diluted, it is improbable that these molecules are in one confocal spot by chance. This can only be the case if they are bound to the same protein molecule, again verifying that the protein was successfully labeled.

WS-TDI as a Membrane Marker. Labeling of Liposomes. Measurements with Pluronic P123 or CTAB in water solutions show that the aggregation of WS-TDI can be strongly reduced above the CMC and strong fluorescence can be achieved. This leads to the idea that WS-TDI can be used for labeling membranes and compartments consisting of membranes such as liposomes, endosomes, and so forth. WS-TDI is nonfluorescent in water solution due to the strong formation of H-aggregates, whereas, in the presence of membranes, WS-TDI becomes monomeric and strongly fluorescent. In this way, membranes can be labeled by incorporation of the dye.

To test this hypothesis, the phospholipidic membrane of artificial liposomes with a diameter of 173 nm (measured by light scattering) was used as a straightforward test system. The fluorescent probe was dissolved in water and added to a suspension of preformed liposomes with gentle mixing. The ratio of lipid-to-fluorescent probe was greater than 300:1 to prevent changes in the liposome membrane structure. The suspension was left for 1 h to ensure complete incorporation of the probe into the lipid bilayer. After purification and dilution of the sample, diffusion of the labeled liposomes in Hepes buffer was monitored by wide-field fluorescence microscopy. Figure 5a shows a frame from an image sequence taken as a movie where each frame is recorded with an exposure time of 100 ms. Bright spots indicating the presence of single liposomes and in some cases small aggregates of liposomes can be seen diffusing freely in solution (Supporting Information, movie 1). Other particles can be seen moving with reduced intensity out of the focal plane of our setup. Fluorescence originates only from liposomes that have incorporated WS-TDI, since the possible remaining dye in water solution forms nonfluorescing aggregates. The emission spectrum obtained from the bright spots in Figure 5a is shown in Figure 5b and presents a spectrum that is identical to the fluorescence spectrum of WS-TDI in the presence of Pluronic P123 in Figure 2d. This clearly indicates the presence of WS-TDI attached to or incorporated in the membrane of the liposomes. Even after several months, the liposomes still contained WS-TDI and could be identified by their fluorescence. In summary, WS-TDI can thus be successfully used to label phospholipid membranes.

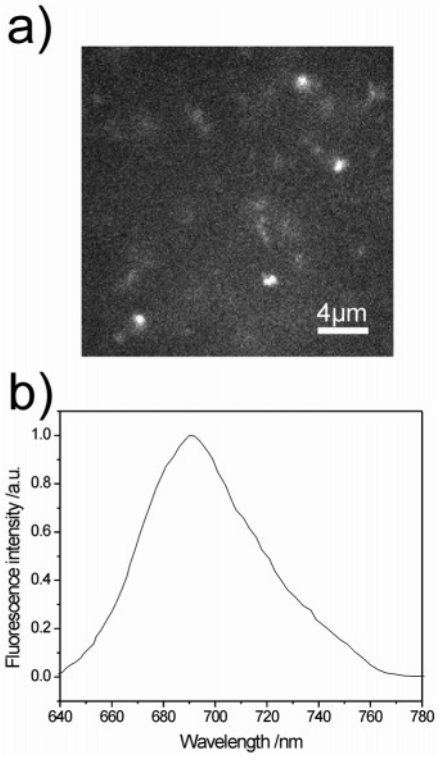

Figure 5. (a) Wide-field image extracted from a movie (100 ms per frame) of WS-TDI-labeled liposomes freely diffusing in Hepes buffer. (b) Fluorescence spectrum acquired with the confocal setup ($\lambda_{ex} = 633$ nm) on a sample of the labeled liposomes 500 times more concentrated than visualized in panel a.

Observation of Membrane Containing Compartments in Living Cells Labeled with WS-TDI. After showing that WS-TDI can label artificial liposomes, we investigated the possibility of labeling membrane containing compartments with WS-TDS in living cells. WS-TDI was compared with two other well-known membrane labeling dyes: Alexa647/dextran and FM 4-64 styryl dye.

Alexa647 is a widely used dye in biology, well-known to yield photostable conjugates.[3] The linking of Alexa647 dye to the hydrophilic polysaccharide dextran creates a conjugate that is often used as a fluid phase marker.[41] This means that Alexa647 bound to dextran can be taken up by the cell in an

(41) Ellinger, I.; Klapper, H.; Fuchs, R. *Electrophoresis* **1998**, *19*, 1154−1161.

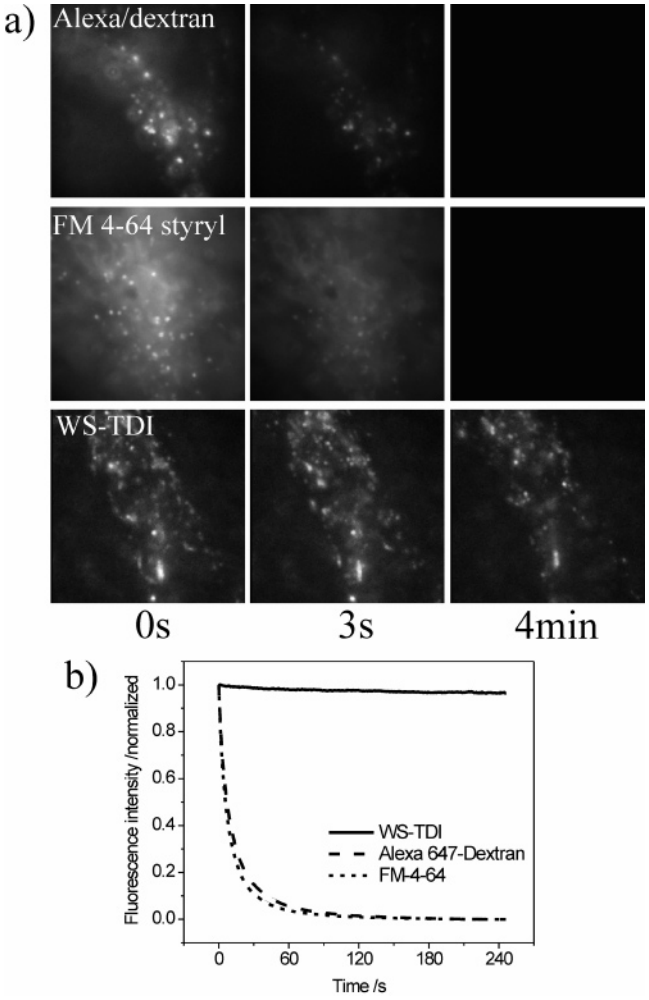

Figure 6. (a) Frames (23 μm $\times$ 23 μm) extracted from three sequences of images of HeLa cells adhered onto a cover glass in PBS and loaded with Alexa647/dextran (top), FM 4-64 styryl dye (middle), and WS-TDI (bottom). The depicted images were acquired after 0 s (left), 3 s (middle), and 4 min (right) of illumination. (b) Plot of the normalized fluorescence intensity as a function of time for the three image sequences.

endocytotic process and thus is contained in endosomes, showing the pathways of these compartments in the living cell.

Using the water-soluble styryl dye, we applied a different mechanism for the imaging of membrane containing cell compartments. Here, the styryl dye is quasi-nonfluorescent in water solution due to its high internal flexibility, but becomes fluorescent when it is incorporated into the membrane. In the membrane, the dye loses most of its internal degrees of freedom, the nonradiative decay channels are blocked, and thus the dye starts to fluoresce. In contrast to the styryl dye, WS-TDI is nonfluorescent in water solution due to the strong formation of H-aggregates, but fluoresces strongly in membranes where it is monomeric.

In dye-uptake experiments, solutions of Alexa647/dextran, styryl dye, and WS-TDI were added to living HeLa cells adherent on a cover glass at 37 °C. The dye concentrations were in each case 4×10^{-6} mol/L (for details, see the Experimental Section). After an incubation period of 40 min, the solutions were washed to remove the excess of dye.

The three dyes could be easily detected by wide-field imaging. Movies were recorded with an integration time of 500 ms per frame over a period of 4 min (Supporting Information, movie 2). Frames taken after 0 s, 3 s, and 4 min of illumination time under identical conditions for all three dyes are shown in Figure 6a.

At the beginning of illumination, the images appear very similar. All three images clearly show many vesicles that were formed at the cell membrane, and the movies show their diffusion within the cell. No significant homogeneous fluorescence background in the cytoplasm was detected for any of the fluorophores, but the best contrast was obtained with WS-TDI. Already after 3 s, fading of intensity due to the photobleaching of Alexa647/dextran and the styryl dye can be clearly observed, and, after a period of about 40 s, nearly no signal of these dyes can be detected. In contrast, WS-TDI-labeled cells still can be beautifully imaged even after 4 min. Additional measurements show that strong fluorescence intensity remains for WS-TDI even after more than 30 min of illumination of the cells, demonstrating again the remarkable photostability of this dye. In Figure 6b, the fading of the images is characterized. The total intensity of the sequence images are plotted versus time. The intensity curves for the three dyes clearly indicate the superior imaging capabilities of the WS-TDI dye due to its high photostability.

Conclusion

The photophysical properties of a new terrylenediimide dye have been investigated. This dye is water-soluble and forms H-type nonfluorescent aggregates in water solution. The addition of surfactants, for example, Pluronic P123 or CTAB, to an aqueous solution of WS-TDI leads to the formation of strongly fluorescent species that can be assigned as monomeric WS-TDI molecules incorporated in micelles.

A single molecule study showed a much higher photostability of WS-TDI in comparison with other well-known water-soluble dyes such as oxazine-1, sulforhodamine B, or a similar perrylendiimide derivative. Furthermore, labeling of a single protein such as avidin has been demonstrated, and the properties of single WS-TDI-labeled avidin molecules have been characterized by FCS and photostability measurements.

The uptake of WS-TDI in liposomes and in living HeLa cells demonstrates the outstanding capability of the WS-TDI to label artificial and natural lipid membrane containing compartments. To our knowledge, there is no other dye that can image the trafficking of, for example, endosomes in living cells over such a long period with such a high brilliance.

In summary, the possibility to excite WS-TDI efficiently in the far red of the visible spectrum (650 nm) avoiding autofluorescence in living cells, the extremely high photostability combined with a good fluorescence quantum yield allowing long observation periods, and the affinity to lipophilic environments make WS-TDI a unique dye for biological applications.

Acknowledgment. We thank Wolfgang Marquardt for experimental assistance with the single molecule photostability measurements and Dr. Martin Hossann for providing the liposomes. We thank the DFG and SFB 486 for financial support.

Supporting Information Available: Movie 1: Labeled liposomes freely diffusing in solution. Movie 2: Live-cell imaging of fluorescently labeled vesicles in HeLa cells using Alexa 647/dextran (left), FM 4-64 styryl dyes (middle), and WS-TDI (right). This material is available free of charge via the Internet at http://pubs.acs.org.

JA0588104